Response of ambient BC concentration across the Indian region to the nation-wide lockdown: results from the ARFINET measurements of ISRO-GBP

Mukunda M. Gogoi[1], S. Suresh Babu[1], B. S. Arun[1,19], K. Krishna Moorthy[2], A. Ajay[3,20], P. Ajay[4], Arun Suryavanshi[5], Arup Borgohain[6], Anirban Guha[7], Atiba Shaikh[8], Binita Pathak[4], Biswadip Gharai[9], Boopathy Ramasamy[10], G. Balakrishnaiah[13], Harilal B. Menon[8], Jagdish Chandra Kuniyal[11], Jayabala Krishnan[12], K. Rama Gopal[13], M. Maheswari[12], Manish Naja[14], Parminder Kaur[7], Pradip K. Bhuyan[4], Pratima Gupta[15], Prayagraj Singh[16], Priyanka Srivastava[14], R. S. Singh[17], Ranjit Kumar[15], Shantanu Rastogi[16], Shyam Sundar Kundu[6], Sobhan Kumar Kompalli[1], Subhasmita Panda[10], Tandule Chakradhar Rao[13], Trupti Das[10] and Yogesh Kant[18]

[1]Space Physics Laboratory, Vikram Sarabhai Space Centre, Thiruvananthapuram 695 022, India
[2]Centre for Atmospheric and Oceanic Sciences, Indian Institute of Science, Bengaluru 560 012, India
[3]Divecha Centre for Climate Change, Indian Institute of Science, Bengaluru 560 012, India
[4]Centre for Atmospheric Studies, Dibrugarh University, Dibrugarh 786 004, India
[5]Regional Remote Sensing Centre, Indian Space Research Organisation, Nagpur 440 033, India
[6]North Eastern – Space Application Centres, Shillong 793 103, India
[7]Department of Physics, Tripura University, Suryamaninagar, Agartala 799 022, India
[8]Department of Marine Sciences, Goa University, Goa 403 206, India
[9]National Remote Sensing Centre, Indian Space Research Organisation, Hyderabad 500 037, India
[10]Indian Institute of Mineral and Materials Technology, Bhubaneswar 751 013, India
[11]G. B. Pant Institute of Himalayan Environment and Development, Kullu 175 126, India
[12]Tamil Nadu Agricultural University, Coimbatore 641 003, India
[13]Sri Krishna Devaraya University, Anantapur 515 003, India
[14]Aryabhatta Research Institute of Observational Sciences, Nainital 263 002, India
[15]Department of Chemistry, Dayalbagh Educational Institute, Agra 282 005, India
[16]Department of Physics, D.D.U. Gorakhpur University, Gorakhpur 273 009, India
[17]Department of Chemical Engineering, IIT-BHU, Varanasi 221 005, India
[18]Indian Institute of Remote Sensing, Indian Space Research Organisation, Dehradun 248 001, India
[19]Research Centre, University of Kerala, Thiruvananthapuram 695 034, India
[20]Department of ECE, Hindustan Institute of Technology and Science, Chennai 603 103, India

In this study, we assess the response of ambient aerosol black carbon (BC) mass concentrations and spectral absorption properties across Indian mainland during the nation-wide lockdown (LD) in connection with the Coronavirus Disease 19 (COVID-19) pandemic. The LD had brought near to total cut-off of emissions from industrial, traffic (road, railways, marine and air) and energy sectors, though the domestic emissions remained fairly unaltered. This provided a unique opportunity to delineate the impact of fossil fuel combustion sources on atmospheric BC characteristics. In this context, the primary data of BC measured at the national network of aerosol observatories (ARFINET) under ISRO-GBP are examined to assess the response to the seizure of emissions over distinct geographic parts of the country. Results indicate that average BC concentrations over the Indian mainland are curbed down significantly (10–40%) from pre-lockdown observations during the first and most intense phase of lockdown. This decline is significant with respect to the long-term (2015–2019) averaged (climatological mean) values. The drop in BC is most pronounced over the Indo-Gangetic Plain (>60%) and north-eastern India (>30%) during the second phase of lockdown, while significant reduction is seen during LD1 (16–60%) over central and peninsular Indian as well as Himalayan and sub-Himalayan regions. Despite such a large reduction, the absolute magnitude of BC remained higher over the IGP and north-eastern sites compared to other parts of India. Notably, the spectral absorption index of aerosols changed very little over most of the locations, indicating the still persisting contribution of fossil-fuel emissions over most of the locations.

*For correspondence. (e-mail: dr_mukunda@vssc.gov.in)

Introduction

IT is well accepted that the short-lived climate forcing agents, such as atmospheric aerosols, cause significant regional and global climatic impact, in which the role of carbonaceous aerosols (through their impact on radiation, cloud and cryosphere) is unique due to a variety of reasons[1–4]. The short atmospheric lifetime (5–10 days in the lower atmosphere) of these species makes it more challenging to model their spatio-temporal distributions and direct and indirect impact on climate accurately. Another challenge is to delineate the exact sources responsible for severe degradation of the environment and air quality in the real atmosphere due to entwined source and life cycle processes. Over the Indian region, the role of both biomass burning (arising mostly for domestic purposes such as the burning of wood, dung, rice straw, and other such material by the economically weaker sections of the society and seasonal forest fires and stubble burning), as well as extensive fossil fuel burning emissions (from industrial, energy and transport sectors) have competing region-specific impacts. However, experimental delineation of this remains elusive due to the co-existence of the ever-prevailing nature of these multiple sources, making it difficult to delineate the individual contributions to the total BC.

The nationwide lockdown (LD) imposed in India (along with several other countries) in connection with the COVID-19 pandemic resulted near to complete restriction of road, rail, marine and air traffic for nearly 6 weeks duration, in addition to shutting down of most of the industries, commercial and business establishments, malls, cinema halls, educational institutions and government and private establishments with a consequent large reduction in power generation. The most intense phase of the lockdown was from 25 March to 14 April (LD1), followed by gradual relaxation in phases; LD2 until 3 May, LD3 until 17 May and LD4 until 31 May. While several restrictions got removed from LD3 onwards, some of the restrictions are still in place like restrictions on international air travel, full restoration of rail services, the opening of educational institutions, cinema halls, etc. This lockdown, especially LD1 and LD2, being longer than the typical atmospheric lifetimes of aerosols, provided a unique opportunity to examine the impact on their ambient concentrations and how it got recharged in the phased relaxation of the restriction on traffic and industries in the later phases of LD and unlock.

In this paper, we present the results of the above on black carbon (BC) mass concentrations and absorption characteristics across Indian landmass, based on long-term primary data from the Aerosol Radiative Forcing over India Network (ARFINET) of aerosol observatories and the implications are discussed.

Data and methodology

Observational sites and database

Regular BC measurements from 19 observatories, where continuous data are available, have been used for this study. These stations are spread across India, as shown in Figure 1, and represent the regions of the Himalayas and sub-Himalayas, Indo-Gangetic Plain (IGP), eastern, central and peninsular India as delineated in Table 1.

Continuous measurements of BC mass concentrations are made at each of the stations using multi-wavelength Aethalometers (Model: AE-33, AE-31, AE-42; Magee Scientific, USA), which have been periodically inter-compared for their consistency. The instruments work on the principle of filter-based optical attenuation technique[5]. To ensure consistency of BC measurements by different models of Aethalometers, we have adopted the technique reported by Gogoi *et al.*[3], where the data from legacy instruments (AE-31 and AE-42) are compensated for loading effect and then inter-compared with AE-33 (reference) system. More details about the experimental techniques and correction schemes are found elsewhere[3,6,7]. For the sites which are located at higher altitudes having reduced ambient pressures, the measured BC values were corrected further for obtaining true BC mass concentration (M_{BC}) following the procedure adopted by Moorthy *et al.*[8].

$$M_{BC} = M_{BC}* \ [P_0T/PT_0]^{-1}, \tag{1}$$

where $M_{BC}*$ is the instrument measured raw BC mass concentration at ambient conditions and P_0 and P are the standard and ambient pressure, and T_0 and T are the corresponding temperatures.
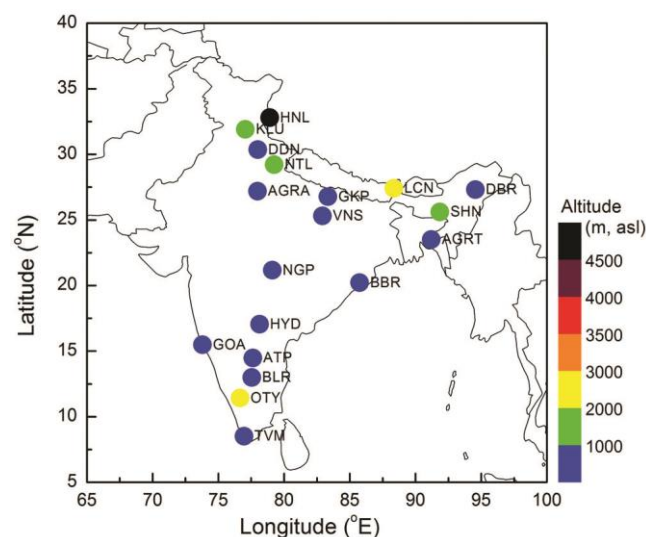

Figure 1. Geographic positions of the ARFINET stations over India, the primary BC data from which are used in the present study. The colour scale indicates the altitude of the stations.

Table 1. Details of the ARFINET stations considered in the present study

| Station	Station code	Longitude (°E)	Latitude (°N)	Altitude (m, a.s.l.)	Region
Hanle	HNL	78.95	32.78	4520	Himalayan and sub-Himalayan
Kullu	KLU	77.1	31.9	1154	
Dehradun	DDN	78.04	30.34	700	
Nainital	NTL	79.3	29.2	1960	
Lachung	LCN	88.4	27.4	2700	
Agra	AGRA	78.02	27.18	169	Indo-Gangetic Plain
Gorakhpur	GKP	83.38	26.75	85	
Varanasi	VNS	82.96	25.3	78	
Agartala	AGRT	91.25	23.5	43	North-eastern and Eastern India
Shillong	SHN	91.91	25.6	1033	
Dibrugarh	DBR	94.6	27.3	111	
Bhubaneswar	BBR	85.8	20.2	78	
Nagpur	NGP	79.15	21.15	300	Central and Peninsular India
Hyderabad	HYD	78.18	17.03	640	
Bengaluru	BLR	77.59	12.97	960	
Goa	GOA	73.83	15.46	70	
Anantapur	ATP	77.67	14.46	331	
Ooty	OTY	76.7	11.4	2520	
Thiruvananthapuram	TVM	77	8.5	2	
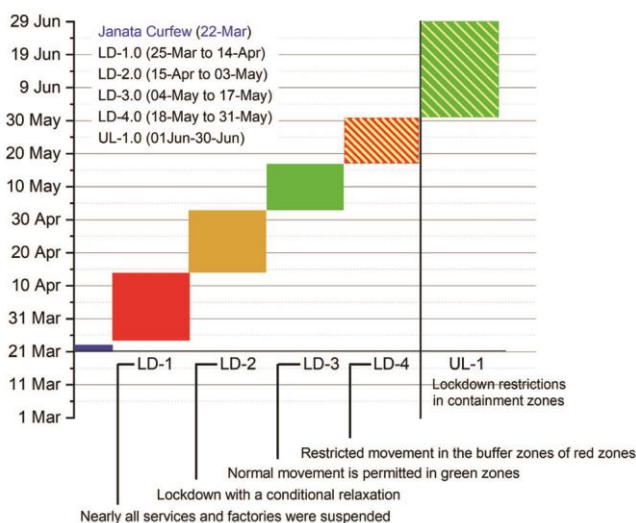
Figure 2. Temporal scales of the lockdown (LD) periods imposed by the Government of India to contain the spread of COVID-19 pandemic. The magnitude of social and travel restrictions varied with the progression of LD from 1 to 4. Nearly all road, rail, air, and marine travel services, along with factories, were suspended during LD1, which is the period of primary interest in the present study.

Lockdown periods and data deduction method

As stated earlier, the first phase of nationwide lockdown (LD1) commenced from 25 March (to 14 April 2020) and was preceded by a 14-hour voluntary Janata curfew on 22 March (Figure 2). During LD1, nearly all services and factories were suspended, restricting social gathering as well as road, passenger train, marine and air travel across the country. However, railway freight operations to transport essential goods were continued. During the second phase (LD2), conditional relaxations were imple-

mented after 20 April for the regions where the infection has been contained or was minimal. This phase continued till 3 May 2020. In the third phase (LD3) from 4 to 17 May 2020, more relaxation of the vehicular movement was put in place, allowing movement of people and material through rail and road (though only on restricted timings), and air services were operated in a modest way as special cases. Offices and industries were opened with about 50% capacity, while other restrictions continued. The relaxations were increased during the 4th phase (LD4: 18–31 May 2020). At the end of LD4, the restrictions were lifted (termed as 'Unlock-1') in most of the areas, and traffic was mostly restored normal, except for a ban during night-time.

In view of the above, we examined the impacts of these on BC by considering the data in the following four distinct time segments:

(i) Pre-LD (A), 4–17 March 2020: This is chosen as the reference pre-lockdown periods for which characteristics of BC concentrations are examined till 7-days before lockdown.

(ii) Pre-LD (B), 18–24 March 2020: This period is chosen separately to understand the impact of Janata curfew on 22 March 2020, in addition to understanding the pre-lockdown concentrations of BC during the previous week of lockdown.

(iii) LD1 (A), 25–31 March 2020: Data for this period is examined separately during the first week of LD1 to delineate the rapid response of the complete cut-off of the emission sources as well as the impact of residual BC in the atmosphere emitted earlier, considering the typical residence time of BC ~ 5–10 days.

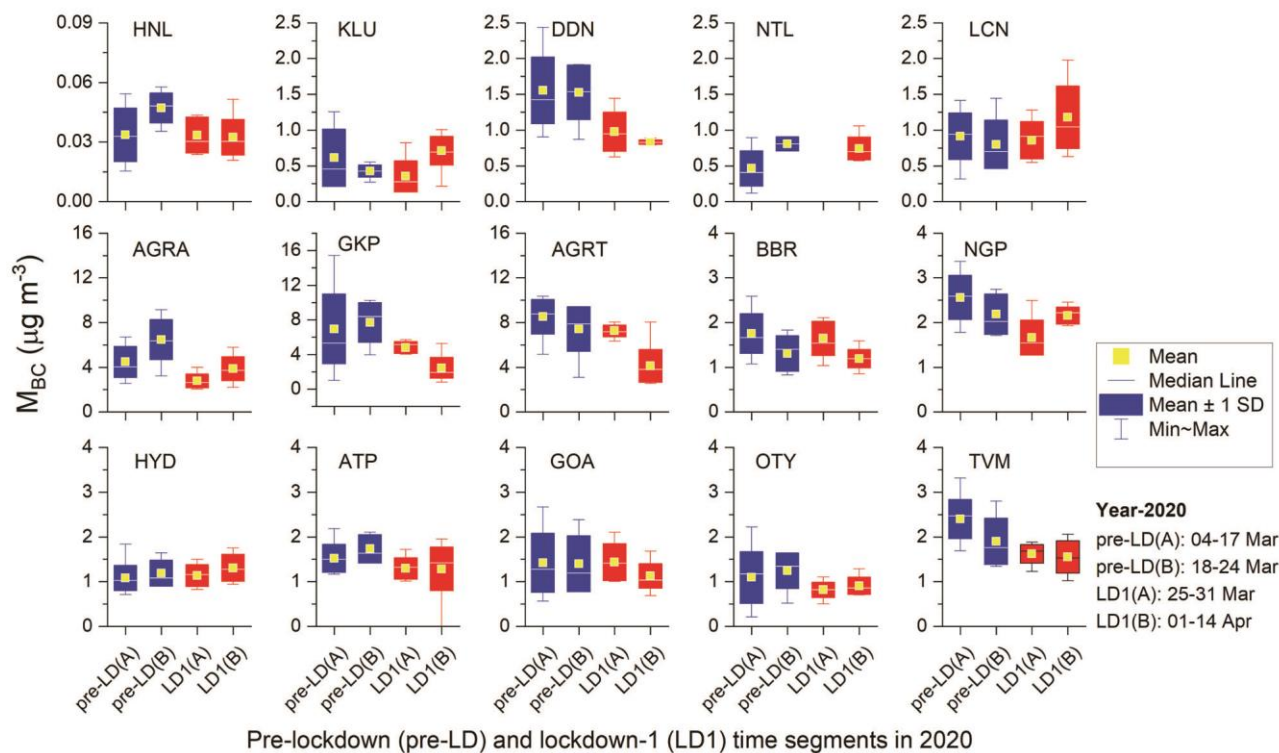(iv) LD1 (B), 1–14 April 2020: This period is chosen to be ideal for a complete understanding of the impact

Figure 3. Distribution of the average values of BC concentrations during two distinct periods of lockdown-1 [LD1(A) and LD1(B)] with reference to the pre-lockdown (pre-LD) values, which cover the periods: (i) pre-LD(A): 4–17 March 2020 (till 7-days before LD1), (ii) pre-LD(B): 18–24 March 2020 (during previous week of LD1), (iii) LD1(A): 25–31 March 2020 (during the first week of LD1) and (iv) LD1(B): 1–14 April 2020 (during the second and third week of LD1). The box shows the standard deviations, while whisker is indicative of the minimum and maximum values of BC.

of lockdown after the first week of LD1, during which the residual BC from fossil fuel sources is expected to be highly subdued.

In addition to the above, we have considered continuous BC data collected for the period from January to May 2020 and examined its features with the climatological mean for the same period estimated using data for the previous five years (2015–2019), which was considered as a reference for the normal conditions.

Results and discussions

BC concentrations before and during LD1

We examine the impact of the phased lockdown on ambient BC mass concentration at different locations in the Box and Whisker plot in Figure 3. Despite the large spatial heterogeneity, which is to be expected due to the diverse nature and strength of the sources across the country, almost all stations show a significant decline in BC concentration through the entire phase of LD1 (25 March–14 April 2020) in comparison to the values that existed prior to the lockdown (4–24 March 2020); half of the stations showed increased reduction during the second

half of the LD1. Until 7-days before lockdown, BC concentration as high as $8.72 \pm 5.19 \ \mu g \ m^{-3}$ was observed at AGRT in north-eastern India (NEI), followed by AGRA ($\sim 5.5 \pm 3.1 \ \mu g \ m^{-3}$) in IGP, whereas the lowest values ($<1.5 \ \mu g \ m^{-3}$) were observed in the Himalayan stations. The maximum values of BC in the IGP and NEI exceeded $10 \ \mu g \ m^{-3}$. Moderate BC ($<3 \ \mu g \ m^{-3}$) prevailed in peninsular India. This pattern is generally consistent with what has been reported in the normal years. Subsequently, BC concentrations were reduced to $<4 \ \mu g \ m^{-3}$ in the NEI and IGP during LD1. The absolute concentrations of BC during LD1 is $<0.5 \ \mu g \ m^{-3}$ over the Himalayan and peninsular Indian sites.

Thus, in general, there has been a significant decrease in the ambient BC concentration across India during the intense phase of the lockdown (LD1). Some deviations were seen at KLU, LCN and HYD, where the BC concentrations though decreased during the first week of LD1, subsequently the values increased during the second half of LD1 with BC higher than the pre-LD values. The increase in BC during the second half of LD1 can be attributed to local sources only as the air mass trajectories or the regional circulation is not supporting the transport of BC from elsewhere during this period.

The overall change in BC during LD1 from the pre-lockdown levels at different stations differed, as can be

Table 2. Percentage change in BC concentration from pre-lockdown (pre-LD) to lockdown-1 (LD-1) period. The colour bar shows different ranges of the percentage change in BC. The absolute change in BC is also shown in the last column

Stations	Percentage change in BC from pre-LD to LD1	Absolute change (ng m^{-3})
HNL	31.4	14.7
NTL	8.3	67.3
DDN	45.5	694.5
KLU	67.5	286.7
LCN	47.7	380.3
AGRA	40.3	2604.3
GKP	68.3	5252.2
AGRT	44.6	3307.7
BBR	8.7	113.1
NGP	1.4	29.6
HYD	9.8	116.4
BLR	51.8	2510.0
ATP	26.0	449.3
GOA	19.6	273.0
OTY	27.1	335.5
TVM	18.5	351.1

0–10%	10–20%	20–30%	30–40%	40–70%

seen from Table 2. The change (decrease) was highest at GKP (68.3%) in the IGP with an absolute reduction in BC concentration to as low as 2.43 µg m^{-3} during LD1, whereas decrease in BC during LD1 was lowest at NGP. It is interesting to note that there was a significant decrease in BC even at the remotest station Hanle (though the magnitude is small), despite its highly subdued anthropogenic activities. This decrease might represent the reduction in transported BC from the valleys.

Deviations from the climatological mean

As the lockdown spanned the period when the synoptic meteorology is in a transition from the dry winter conditions, with isolated pre-monsoon showers (as shown in Supplementary Figure) occurring in different parts of the country, the observations in Figure 3 would have the imprint of the seasonal transformation of BC sources and atmospheric dynamical processes, at least at some of the stations, in addition to the impact of the cessation of various emission sources during lockdown. With a view to delineating the impacts of the LD from the combined effects, we have considered the climatological average BC values for the period January to May by making use of the long-term measurements from 2015 to 2019 and considered this as the reference BC level prevailing during this period under normal conditions (i.e. in the absence of a LD). Figure 4 shows the time series of daily mean BC mass concentrations at each of these stations for the year 2020, against the corresponding time series of normal-state reference levels. It clearly shows the unambiguous impact of the lockdown across the entire region, with a stronger signature at urban locations than in rural and remote locations. Even the Himalayan stations depicted a significant reduction in BC during the lockdown. In general, the springtime enhancement of BC in the Himalayas is a consistent phenomenon, as has been re-

ported earlier[9–11]. This is also explicit from the historical data shown in the present study. However, not only that, spring time enhancements are suppressed during the LD in 2020, there is a significant decrease as well (as seen from the two top panels on the left and right of Figure 4). As long-range transport from the IGP contributes significantly to the BC loading at these high-altitude stations, the large drop in BC loading over the Himalayan stations during 2020 is a clear evidence of the impact of the reduced emissions over the plains.

This is further vindicated by Figure 5, in which we show the percentage decrease in BC from its climatological mean normal-state values (we call this the anomaly due to LD) for different phases of lockdown as a contour plot. In its top panel, we also show the average values of BC during the entire period of lockdown (i.e. LD1 to LD4). The figure reveals the significant impact across the entire region, being most pronounced over the IGP and eastern Indian stations during the LD2 phase. This is attributed to the continued suppression of emissions due to the prolonged lockdown and the absence of 'recharging'. The influence of relaxation is reflected from LD3 onwards, as the atmosphere gets gradually charged with BC, and the strength of the LD anomaly decreases gradually and becomes highly localized by LD4. The only exception to this has been the urban location of HYD, the reasons for which need a separate investigation. Quantitatively, the LD anomaly during LD2 is >60% over the IGP, while it varied between 26% and 66% over the Himalayan/sub-Himalayan regions (where the average BC level itself is low) and 22% to 59% over the northeastern and eastern locations of India. In the central and peninsular region, the highest decline of BC occurred at NGP and ATP (~60%) and least at southern high-altitude site OTY (~16%).

Despite this spatial pattern of the LD anomaly, the absolute magnitude of BC (as shown by the histograms in
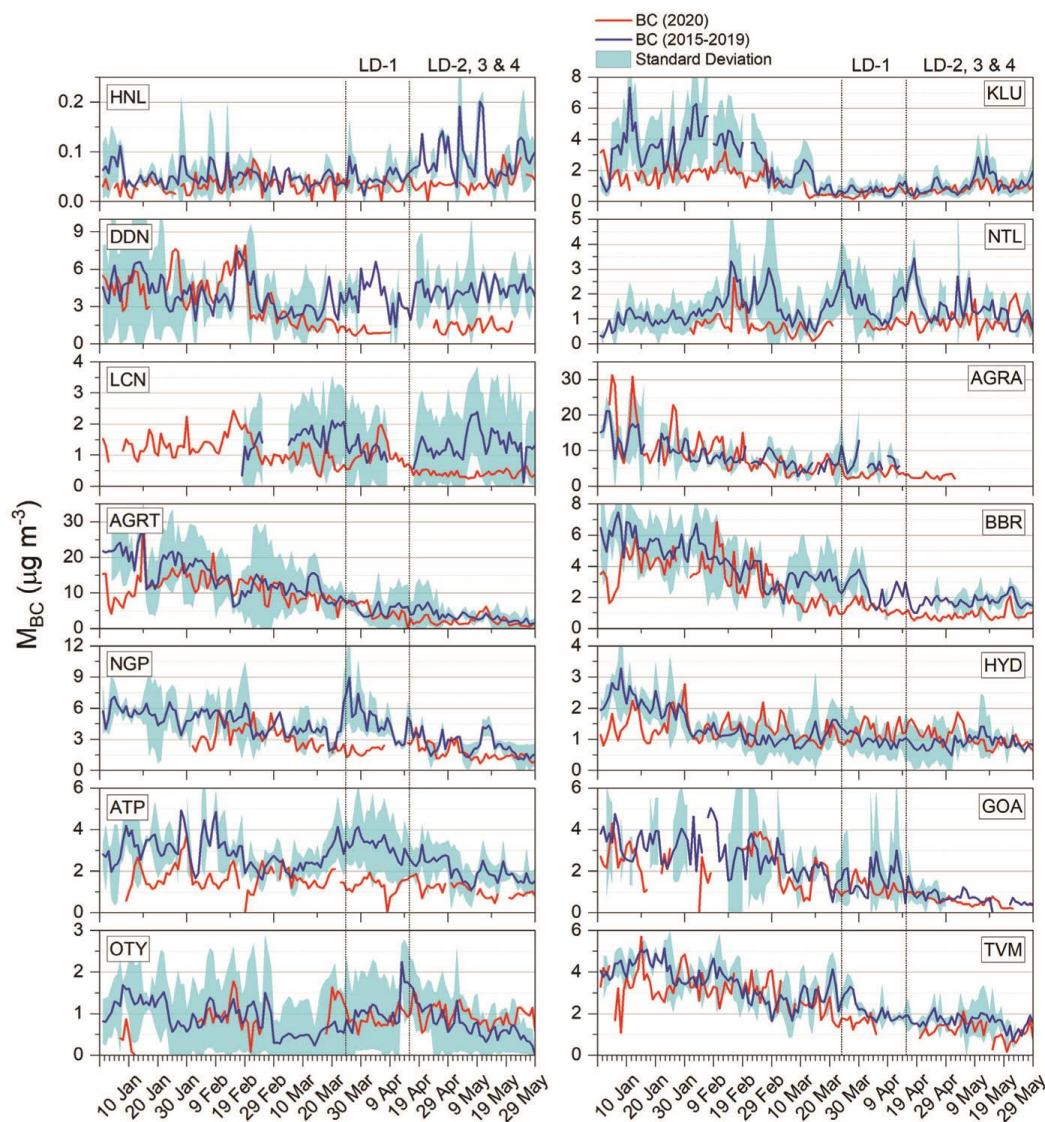
Figure 4. Day to day variability of BC mass concentrations during the year 2020 (for the period from January to May), along with the average values of the years 2015–2019. The shaded colour indicates the standard deviations of the mean of the historical values.

the top panel of Figure 5) remained higher over the IGP and north-eastern sites of India compared to other regions. This indicates the still persisting contribution of fossil-fuel emissions to the ambient BC over these sites where the impact of several other sources (such as industries, thermal power plants or brick kilns), in addition to that of vehicular traffic, is prominent. Interestingly, Himalayan foothills, IGP and north-eastern part of India also showed a significant BC drop compared to the locations such as ATP, BLR, OTY and TVM, indicating larger decline in BC over the places where there are abundant non-transport fossil fuel emission sources (e.g. industries, thermal power plants, etc.) compared to the regions where the transport sector is a major contributor. Accordingly, the efficiency of BC removal from the

atmosphere may vary from heavily loaded region to the least. Quantification of such gradients is important for climate impact studies, especially in the light of the elevated heat pump hypothesis[12], which has demonstrated that perturbation to the regional monsoon through this mechanism is strongly dependent on the meridional gradient in elevated aerosol absorption.

On a regional perspective, the time series of the regional mean (daily) values of BC (averaged over all the stations for the year 2020 and for the climatological period 2015–2019) is shown in Figure 6. It is evident that the reduction in BC during LD1 (37.9%) and LD2 (52.5%), with respect to their pre-LD values, are quite unusual as against the corresponding values (11.8% and 23.7%) in climatological trend in BC over India. The

depletion of BC from the climatological mean value (anomaly) is sharp during LD1 (50%) and LD2 (55%). This indicates that the effect of lockdown is much higher than the seasonal change in BC over India.
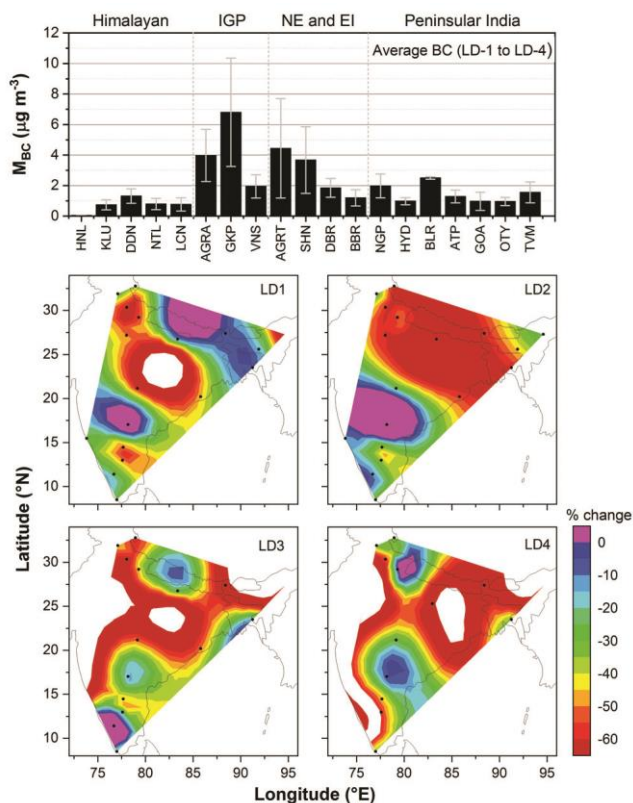

Figure 5. Change (in percentage) in the magnitude of BC concentrations during the lockdown periods (LD1, LD2, LD3 and LD4) in comparison to the average values of the corresponding period of the year 2015–2019. The top panel shows average values of BC during the entire period of lockdown (i.e. LD1 to LD4).
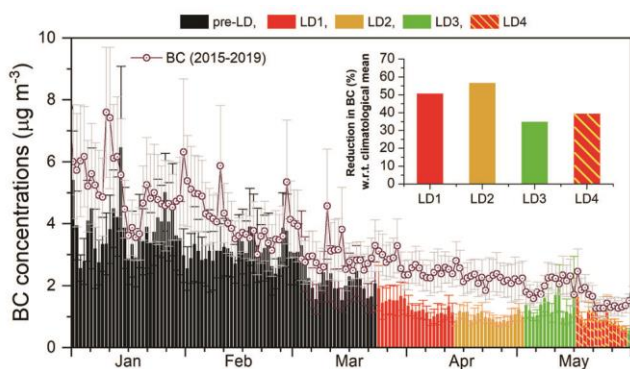

Figure 6. Time series of the daily mean values of BC (shown by the coloured histograms) over India (averaged for all the stations) during January–May 2020, shown in different colours for pre-LD, LD1, LD2, LD3 and LD4 periods. Corresponding multi-year (2015–2019) averaged time series of daily mean BC over India are also shown (open circles). The vertical bars through the means are standard errors. The inset figure shows the reduction (in percentage) in BC during different periods of lockdowns (in 2020) with respect to the corresponding long-term average (2015–2019) BC.

Similar to BC, a statistically significant decline of $PM_{2.5}$, PM_{10}, NO_2, and CO has been reported[13] across five megacities of India: Delhi, Mumbai, Chennai, Kolkata and Bengaluru during COVID-19 lockdown. The highest decline of $PM_{2.5}$ has been reported at Delhi (41%), followed by Mumbai (33%), Kolkata (23%), Bengaluru (22%) and Chennai (14%) during 25 March to 6 April 2020, in comparison to the pre-lockdown values measured during 10–20 March 2020. A higher depletion rate in the northern part of the country is quite interesting. In our present study also, the highest reduction in BC is seen over the northern and eastern parts of India, along with the Himalayan stations. Mahato *et al.*[14] have also reported nearly fifty percent reductions in PM_{10} and $PM_{2.5}$ concentrations at the north Indian site Delhi during the lockdown period compared to the pre-lockdown values. Air quality studies in 22 different cities at different regions of India have also shown an overall 43%, 31%, 10% and 18% decrease in $PM_{2.5}$, PM_{10}, CO and NO_2 due to the effect of restricted emissions during COVID-19, while showing an increase in O_3 concentrations over most regions[15]. Similarly, based on their observations at Bengaluru, Ajai *et al.* (this issue) have reported a significant (>60%) reduction in BC from fossil fuel emission during LD1 and attributed it to the near-total suspension of traffic (road, rail and air).

Similar reductions in aerosol concentration and improvement in air quality due to lockdown and travel restrictions have been reported over several places across the globe[16,17]. A decline in the levels of $PM_{2.5}$, PM_{10}, SO_2, CO and NO_2 is reported over China[18], reduction in NO, NO_2 and CO concentrations over Brazil[19] and Barcelona[20], etc. Similarly, Otmani *et al.*[21] have shown the reduction in PM_{10}, SO_2, and NO_2 concentrations in Morocco, revealing the impact of long-range transported aerosols on reduced PM_{10} concentrations during the lockdown. In Ecuador, Monserrate and Ruano[22] have reported significant reductions in NO_2 and $PM_{2.5}$ concentrations during the establishment of lockdown measures. Based on high-resolution space-borne data, Bauwens *et al.*[23] have reported reductions in pollution levels over widespread areas in China, Europe, South Korea and the U.S. during January–April 2020. Sicard *et al.*[24] have also reported a substantial reduction (~ 56%) of NO_x in Europe and China. All these reported studies showed positive consequences of air quality during the COVID-19 lockdown and the advantages of actualizing extreme measures to moderate a portion of the anthropogenic sources to implement the air quality controls.

Evaluation of distinct source processes

The spectral variation of BC absorption coefficient (σ_{abs}), usually represented using absorption Angstrom wavelength exponent (α_{abs}), in the relation
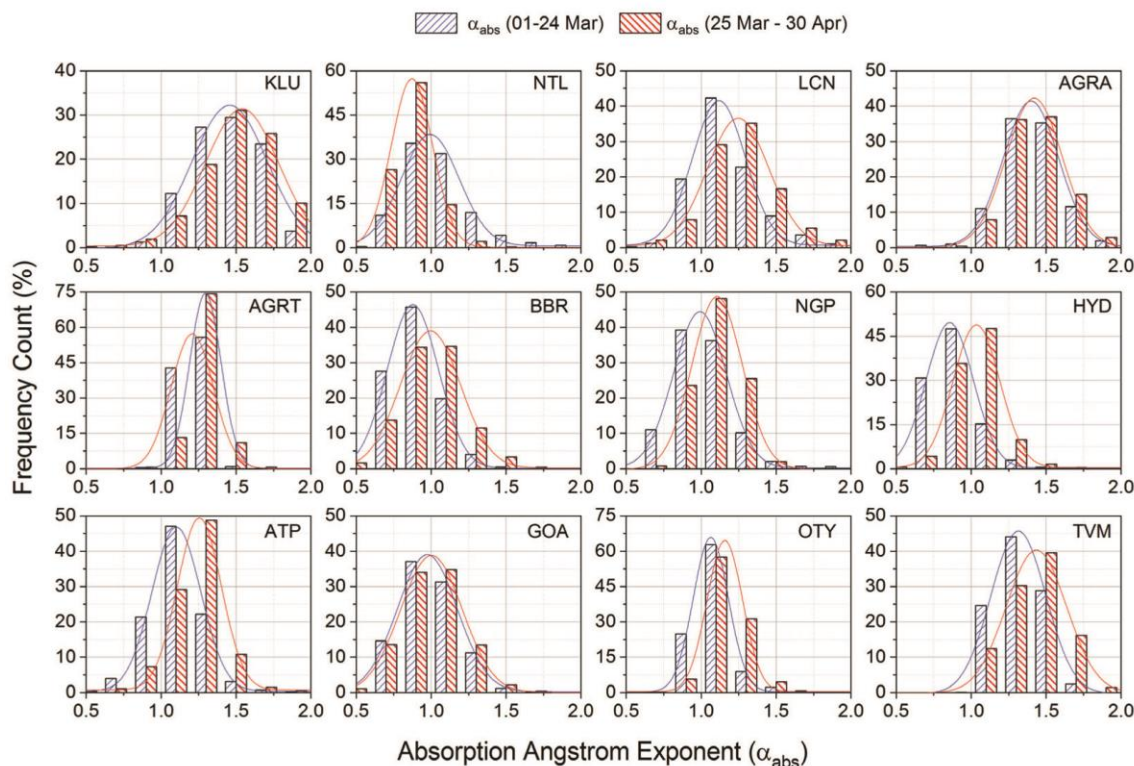
Figure 7. Frequency of occurrences of absorption Angstrom exponent (α_{abs}) during pre-lockdown and lockdown periods.

Table 3. Mean and standard errors of the mean values of absorption Angstrom exponent (α_{abs}) during the pre-lockdown (1–24 March 2020) and lockdown (25 March–30 April 2020) periods

Station	Mean α_{abs} (before lockdown)	Mean α_{abs} (during lockdown)
KLU	1.46 ± 0.04	1.54 ± 0.05
NTL	1.02 ± 0.04	0.88 ± 0.02
LCN	1.17 ± 0.04	1.27 ± 0.04
AGRA	1.41 ± 0.04	1.43 ± 0.03
AGRT	1.20 ± 0.01	1.29 ± 0.02
BBR	0.89 ± 0.03	1.18 ± 0.04
NGP	1.01 ± 0.03	1.09 ± 0.02
HYD	0.87 ± 0.03	1.03 ± 0.02
BLR	1.11 ± 0.04	1.31 ± 0.04
ATP	1.10 ± 0.03	1.23 ± 0.03
GOA	0.96 ± 0.04	1.01 ± 0.03
OTY	1.08 ± 0.02	1.17 ± 0.02
TVM	1.31 ± 0.02	1.43 ± 0.03

$$\sigma_{abs} = \beta\lambda^{-\alpha_{abs}}, \tag{2}$$

where β wavelength-independent constant (that equals to the absorption coefficient at the wavelength $\lambda = 1 \, \mu m$), provides a means to infer the source characteristics of BC; with values of α_{abs} being around 1 for BC aerosols originating from fossil fuel combustion, while for those originating from biomass burning sources show stronger wavelength dependence with $\alpha_{abs} \sim 2$ (refs 25, 26). Values within this range indicate the presence of BC from mixed sources. Clarke *et al.*[27] have reported that α_{abs} peak at 2.1 (1.2–2.2) for biomass burning aerosols and peak close to 1.0 (0.7–1.1) for aerosols from urban pollution.

In the above backdrop, we have examined the frequency of occurrences of α_{abs} for the pre-LD (1–24 March 2020) and LD (25 March–30 April) periods. This is shown in Figure 7, and the average values of α_{abs} prior to lockdown and during lockdown are given in Table 3. The observation shows very little change in α_{abs} over most of the locations except for a few locations such as ATP, BLR and TVM, where vehicular traffic is the major source of fossil fuel-based BC. On the other hand, nearly consistent values of α_{abs} (~1) at some of the locations (such as NTL, BBR, NGP, HYD, GOA and OTY) indicate the persisting impact of fossil fuel sources other than vehicular emission, which influence the absorption spectra of BC but do not significantly contribute to the absolute magnitude of BC concentrations. Similarly, α_{abs} at LCN, KLU, AGRA and AGRT also remains constant, but with steeper BC spectra ($\alpha_{abs} > 1$) during both pre-LD and LD periods. This observation indicates the variability in the relative strength in fossil fuel and bio-fuel sources across the country, having a competing effect in determining the absolute concentrations and spectral signatures of BC at different locations during the lockdown. It is not clear whether the drop in BC at a location is associated with the reduced emissions from the local transport sectors alone. This is because places like the Himalayan foothills,
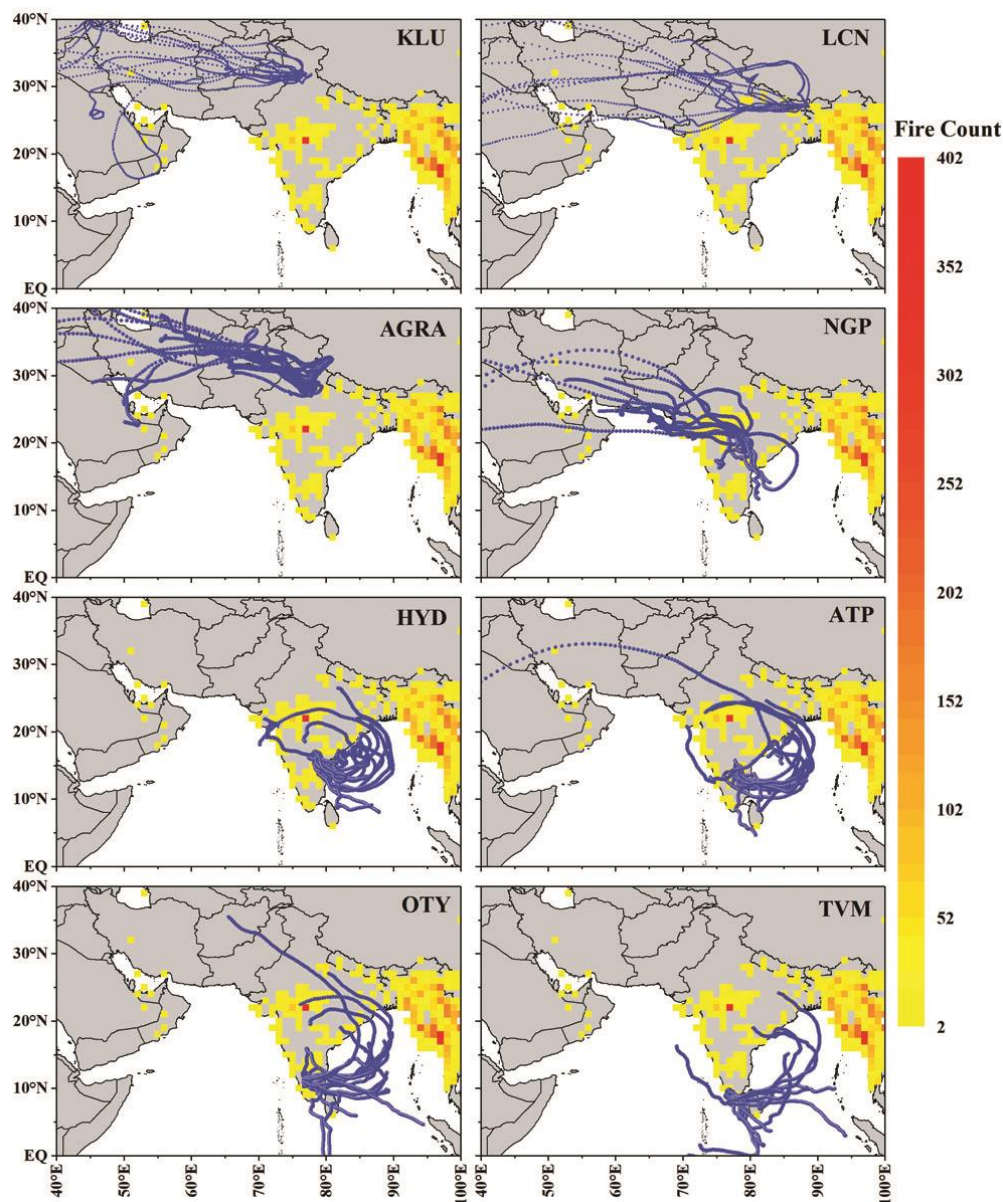
Figure 8. Spatial distribution of MODIS fire counts during the second half of LD1 (period 1–14 April 2020), along with 7-day air mass back trajectories arriving at 500 m AGL at KLU, LCN, AGRA, NGP, HYD, ATP, OTY and TVM, over which the BC concentrations during LD1(B) is higher than the values during LD1(A).

the IGP, northeast region showed a significant drop compared to the locations such as ATP, BLR, OTY, TVM where the transport sector is a major contributor. This suggests that atmospheric lifetime and transport pathways are also a major factor in determining BC loading at any location.

To examine the possible impact of biomass burning sources, regional distribution of fire pixel counts (obtained from MODIS sensor onboard Terra satellite) during LD1, along with 7-days HYSPLIT air mass back trajectories ending at 500 m above ground level, are examined in Figure 8 at a few selected locations (KLU, LCN, AGRA, NGP, HYD, ATP, OTY and TVM) over

which the BC concentrations during LD1(B) is higher than the values during LD1(A) (as depicted in Figure 3). It is evident from the figure that most of these regions experienced moderate to the strong influence of biomass burning sources as the air mass trajectories spend long traverse time over the biomass burning regions before arriving at the receptor sites. For the north Indian sites, the trajectories are mainly confined to the continental regions, while the air mass trajectories pass over the oceanic region of Bay of Bengal before arriving at the receptor sites of peninsular India (viz. HYD, ATP, OTY and TVM). This explains the different behaviour of BC at different locations after the first week of LD1, where the

impact of regional sources of biomass burning aerosols and the associated transport pathways vary from one location to the other.

Apart from the biomass burning sources, the presence of local domestic fire activities can also contribute to the steeper BC spectra. For example, relatively higher values of α_{abs} at KLU and AGRA during pre-lockdown and lockdown periods could be attributed to such activities. Kuniyal et al.[28] have reported the influence of local biomass burning sources like fuel wood for cooking, forest fires, open waste burning, etc. contributing to the high BC concentrations over KLU, in addition to vehicular emissions.

On the other hand, nearly consistent values of α_{abs} close to 1.0 at locations such as NTL, GOA, HYD are indicative of the prevailing BC mainly from fossil fuel sources, but with reduced concentrations during the LD1. At NTL, the background BC is reported to have emitted from the local household usage of fuel, in addition to vehicular emission and transported components from the nearby regions[29]. Similarly, the source of BC over HYD is mainly of fossil fuel (average value of $\alpha_{abs} \sim 1.05 \pm 0.04$ during MAM) rather than biofuel combustion[30]. The present study indicates a consistent value α_{abs} (~1.03 ± 0.16) indicating the presence of fossil fuel components even during the lockdown period. Based on the ground-based and satellite observation along with aerosol reanalysis products, Pandey and Vinoj[31] have shown an unexpected increase (~ +20%) in aerosol optical depth over central India due to increased atmospheric moisture coupled with stagnant circulation condition.

The foregone observations clearly indicate that BC loading at any location is a function of distinct source strength, sink and advection pathways. Even though the observed BC drop during the lockdown reflects its response to cut-off of fossil fuel sources, especially the transport sector, delineating the actual contribution from different emission pathways to total BC load in the atmosphere is difficult without a combination of the observations and modelling. Based on modelling study conducted for March–May 2006, Kumar et al.[32] reported that the anthropogenic emissions contribute 60–95% of the total BC loading in South Asia where BC emissions from residential, industrial, transport and power plant sectors contribute about 61%, 23%, 15% and 1% respectively. The present study indicates that though emissions from industrial and transport sectors reduced significantly during LD, the possible contribution from residential and seasonal biomass burning sources remained significant and played a dominant role in modulating the regional aerosol scenario over India during the COVID-19 lockdown.

Summary and conclusions

We have studied the response of ambient BC concentration across the Indian region during the national lockdown in connection with the COVID-19 pandemic. The major findings of the study are:

- Regional distribution of BC clearly shows the unambiguous impact of the lockdown across the entire region, with a stronger signature at urban locations than at rural and remote locations. The overall change (reduction) from the pre-lockdown levels differed at different stations having the highest decrease at Gorakhpur (68.3%) in the IGP, and the lowest reduction at Nagpur in the central India.
- A spectacular decline of BC during the lockdown periods of 2020, with respect to the five-year average for 2015–2019, is observed across the entire Indian region; being most pronounced over the IGP (>60%) and eastern India during LD2 while central and peninsular India as well as Himalayan and sub-Himalayan regions showed significant decline in BC (16–60%) during LD1.
- The absorption Angstrom exponent showed a very little change over most of the locations (indicating the still persisting contribution of fossil-fuel emissions to the ambient BC) except for a few locations where vehicular traffic is the major source of fossil fuel-based BC, and other sources (such as industries or thermal power plants) do not contribute significantly.
- Airmass back trajectories indicated the influence of advection across biomass burning sources contributing to aerosol loading at a few stations during the lockdown period.

1. Ramanathan, V. and Carmichael, G., Global and regional climate changes due to black carbon. *Nat. Geosci.*, 2008, **1**, 221–227.
2. Bond, T. C. *et al.*, Bounding the role of black carbon in the climate system: a scientific assessment. *J. Geophys. Res. Atmos.*, 2013, **118**, 5380–5552; doi:10.1002/jgrd.50171.
3. Gogoi, M. M. *et al.*, Radiative effects of absorbing aerosols over north-eastern India: observations and model simulations. *J. Geophys. Res. Atmos.*, 2017, 122(2), 1132–1157; doi:10.1002/2016JD025592.
4. Li, G. L., Sun, L., Ho, K. F., Wong, K. C. and Ning, Z., Implication of light absorption enhancement and mixing state of black carbon (BC) by coatings in Hong Kong. *Aerosol Air Qual. Res.*, 2018, **18**, 2753e2763.
5. Lack, D. A., Moosmüller, H., McMeeking, G. R., Chakrabarty, R. K. and Baumgardner, D., Characterizing elemental, equivalent black, and refractory black carbon aerosol particles: a review of techniques, their limitations and uncertainties. *Anal. Bioanal. Chem.*, 2014; doi:10.1007/s00216-013-7402-3.
6. Weingartner, E., Saathof, H., Schnaiter, M., Streit, N., Bitnar, B. and Baltensperger, U., Absorption of light by soot particles: determination of the absorption coefficient by means of Aethalometers. *J. Aerosol Sci.*, 2003, **34**, 1445–1463; doi:10.1016/S0021-8502(03)00359-8.
7. Drinovec, L. *et al.*, The 'dual-spot' Aethalometer: an improved measurement of aerosol black carbon with real-time loading compensation. *Atmos. Meas. Tech.*, 2015, **8**, 1965–1979; doi: 10.5194/amt-8-1965-2015.
8. Moorthy, K. K., Babu, S. S., Sunilkumar, S. V., Gupta, P. K. and Gera, B. S., Altitude profiles of aerosol BC, derived from aircraft

measurements over an inland urban location in India. *Geophys. Res. Lett.*, 2004; doi:10.1029/2004GL021336. L1B2103.

9. Babu, S. S. *et al.*, High altitude (~4520 m amsl) measurements of black carbon aerosols over western trans-Himalayas: seasonal heterogeneity and source apportionment. *J. Geophys. Res. Atmos.*, 2011, **116**(24), 1–15; doi:10.1029/2011JD016722.

10. Gogoi, M. M. *et al.*, Physical and optical properties of aerosols in a free tropospheric environment: Results from long-term observations over western trans-Himalayas. *Atmos. Environ.*, 2014, **84**, 262–274.

11. Arun, B. S., Aswini, A. R., Gogoi, M. M., Hegde, P., Kompalli, S. K., Sharma, P. and Babu, S. S., Physico-chemical and optical properties of aerosols at a background site (~4 km a.s.l.) in the western Himalayas. *Atmos. Environ.*, 2019, doi:10.1016/j.atmosenv.2019.1170.

12. Lau, K. M., Kim, M. K. and Kim, K. M., Aerosol induced anomalies in the Asian summer monsoon – the role of the Tibetan Plateau. *Clim. Dyn.*, 2006, **26**, 855–864; doi:10.1007/s00382-006-0114-z.

13. Jain, S. and Sharma, T., Social and travel lockdown impact considering coronavirus disease (COVID-19) on air quality in megacities of India: present benefits, future challenges and way forward. *Aerosol Air Qual. Res.*, 2020; doi:10.4209/aaqr.2020.04.0171.

14. Mahato, S., Pal, S. and Ghosh, K. G., Effect of lockdown amid COVID-19 pandemic on air quality of the megacity Delhi, India. *Sci. Total Environ.*, 2020; doi:10.1016/j.scitotenv.2020.139086.

15. Sharma, S., Zhang, M., Anshika, Gao, J., Zhang, H. and Kota, S. H., Effect of restricted emissions during COVID-19 on air quality in India. *Sci. Total Environ.*, 2020; doi:10.1016/j.scitotenv.2020.138878.

16. Bao, R. and Zhang, A., Does lockdown reduce air pollution? Evidence from 44 cities in northern China. *Sci. Total Environ.*, 2020; doi:10.1016/j.scitotenv.2020.139052.

17. Saadat, S., Rawtani, D. and Hussain, C. M., Environmental perspective of COVID-19. *Sci. Total Environ.*, 2020; doi:10.1016/j.scitotenv.2020.138870.

18. Xu, K., Cui, K., Young, L. H., Hsieh, Y. K., Wang, Y. F., Zhang, J. and Wan, S., Impact of the COVID-19 event on air quality in central China. *Aerosol Air Qual. Res.*, 2020, **20**, 915–929; doi:10.4209/aaqr.2020.04.0150.

19. Nakada, L. Y. K. and Urban, R. C., COVID-19 pandemic: Impacts on the air quality during the partial lockdown in São Paulo state, Brazil. *Sci. Total Environ.*, 2020, **730**, 139087; doi:10.1016/j.scitotenv.2020.139087.

20. Tobías, A. *et al.*, Changes in air quality during the lockdown in Barcelona (Spain) one month into the SARS-CoV-2 epidemic. *Sci. Total Environ.*, 2020, **726**, 138540; doi:10.1016/j.scitotenv.2020.138540.

21. Otmani, A., Benchrif, A., Tahri, M., Bounakhla, M., Chakir, E. M., Bouch, M. E. and Krombi, M., Impact of COVID-19 lockdown on PM_{10}, SO_2 and NO_2 concentrations in Salé City (Morocco). *Sci. Total Environ.*, 2020; doi:10.1016/j.scitotenv.2020.139541.

22. Monserrate, M. A. Z. and Ruano, M. A., Has air quality improved in Ecuador during the COVID-19 pandemic? A parametric analysis. *Air Quality Atmos. Health*, 2020; doi:10.1007/s11869-020-00866-y.

23. Bauwens, M. *et al.*, Impact of coronavirus outbreak on NO_2 pollution assessed using TROPOMI and OMI observations. *Geophys. Res. Lett.*, 2020; doi:10.1029/2020GL087978.

24. Sicard, P. *et al.*, Amplified ozone pollution in cities during the COVID-19 lockdown. *Sci. Total Environ.*, 2020; doi:10.1016/j.scitotenv.2020.139542.

25. Schnaiter, M., Horvath, H., Mohler, O., Naumann, K.-H., Saatho, H. and Schock, O. W., UV-VIS-NIR spectral optical properties of soot and soot-containing aerosols. *J. Aerosol Sci.*, 2003, **34**, 1421–1444.

26. Kirchstetter, T. W. and Novakov, T., Evidence that the spectral dependence of light absorption by aerosols is affected by organic carbon. *J. Geophys. Res.*, 2004, **109**, D21208; doi:10.1029/2004JD004999.

27. Clarke, A. *et al.*, Biomass burning and pollution aerosol over North America: Organic components and their influence on spectral optical properties and humidification response. *J. Geophys. Res.*, 2007, **112**, D12S18; doi:10.1029/2006JD007777.

28. Kuniyal, J. C., Sharma, M., Chand, K. and Mathela, C. S., Water soluble ionic components in particulate matter (PM_{10}) during high pollution episode days at Mohal and Kothi in the North-Western Himalaya, India. *Aerosol Air Qual. Res.*, 2015, **15**, 529–543.

29. Joshi, H., Naja, M., David, L. M., Gupta, T., Gogoi, M. M. and Babu, S. S., Absorption characteristics of aerosols over the central Himalayas and its adjacent foothills. *Atmos. Res.*, 2019, **233**, 104718; doi:10.1016/j.atmosres.2019.104718.

30. Dumka., U. C., Manchanda, R. K., Sinha, P. R., Sreenivasan, S., Moorthy, K. K. and Babu, S. S., Temporal variability and radiative impact of black carbon aerosol over tropical urban station Hyderabad. *J. Atmos. Sol. Terr. Phys.*, 2013; doi:10.1016/j.jastp.2013.08.003.

31. Pandey, S. K. and Vinoj, V., Surprising increase in aerosol amid widespread decline in pollution over India during the Covid19 Lockdown, EarthArXiv., 2020; doi:10.31223/osf.io/5kmx2.

32. Kumar, R. *et al.*, Sources of black carbon aerosols in South Asia and surrounding regions during the integrated campaign for aerosols, gases and radiation budget (ICARB). *Atmos. Chem. Phys.*, 2015, **15**(10), 5415–5428; doi:10.5194/acp-15-5415-2015.